ELSEVIER

Journal of Fluids and Structures 24 (2008) 720–731

JOURNAL OF FLUIDS AND STRUCTURES

www.elsevier.com/locate/jfs

Spectrographic analysis for the modal testing of nonlinear aeroelastic systems ☆

C.C. Marsden, S.J. Price*

Department of Mechanical Engineering, McGill University, 817 Sherbrooke Street West, Montréal, Que., Canada H3A 2K6

Received 2 October 2006; accepted 6 November 2007
Available online 2 January 2008

Abstract

The spectrograph is a signal-processing tool often used for the frequency domain analysis of time-varying signals. When the signal to be analyzed is a function of time, the spectrograph represents the frequency content of the signal as a sequence of power spectra that change with time. In this paper, the usefulness of the technique is demonstrated in its application to the analysis of the time history response of a nonlinear aeroelastic system. The aeroelastic system is modelled analytically as a two-dimensional, rigid airfoil section free to move in both the bending and pitching directions and possessing a rigid flap. The airfoil is mounted by torsional and translational springs attached at the elastic axis, and the flap is used to provide the forcing input to the system. The nonlinear system is obtained by introducing a freeplay type of nonlinearity in the pitch degree-of-freedom restoring moment. The airfoil is immersed in an aerodynamic flow environment, modelled using incompressible thin airfoil theory for unsteady oscillatory motion. The equations of motion are solved using a fourth-order Runge–Kutta numerical integration technique to provide time-history solutions of the response of the airfoil in the pitch and plunge directions. Time-histories are obtained for the nonlinear responses of the linear and nonlinear aeroelastic systems to a sine-sweep input. The time-histories are analyzed using the spectrographic technique, and the frequency content of the response is plotted directly as a function of the input frequency. Results show that the combination of the sine-sweep input with the spectrographic analysis permits a unique insight into the behavior of the nonlinear system with a minimum of testing. It is shown that the frequency of the nonlinear system response is a function of the input frequency and one other characteristic frequency that can be associated with the limit cycle oscillations of the same nonlinear system subject to a transient input.

Keywords: Aeroelasticity; Spectrographic analysis; Nonlinear dynamics; Signal processing; Frequency domain analysis

1. Introduction

Modal testing is often employed in the determination of natural frequencies and damping levels in aircraft structures. In the forced response to a sine-sweep, a time-varying sinusoidal exciting force is applied over a range of frequencies

☆ An earlier version of this paper was presented in the 7th FSI, AE & FIV + N Symposium, held within the 2006 PV & P Conference in Vancouver, BC, Canada.

*Corresponding author. Tel.: +1 514 398 6291; fax: +1 514 398 7365.
E-mail address: stuart.price@mcgill.ca (S.J. Price).

0889-9746/$ - see front matter © 2007 Elsevier Ltd. All rights reserved.
doi:10.1016/j.jfluidstructs.2007.11.003

Nomenclature

a_h	nondimensional distance measured from the airfoil mid-chord to the elastic axis
b	airfoil semi-chord
c_h	translational viscous damping coefficient in plunge
c_α	torsional viscous damping coefficient in pitch
c_β	nondimensional distance of the flap hinge from the airfoil mid-chord
h	plunge displacement of the airfoil
I_α	moment of inertia of the airfoil/flap about the elastic axis
K_h	linear structural stiffness in plunge
K_α	linear structural stiffness in pitch
m	the combined aileron/flap mass per unit span
m_β	the flap mass per unit span
m_0	restoring moment preload for bilinear spring
r_α	nondimensional radius of gyration of the airfoil/flap about the elastic axis
U	nondimensional free stream velocity, $V/b\omega_\alpha$
U^*	nondimensional linear flutter velocity
V	free stream velocity
x_α	nondimensional distance from the airfoil center of mass to the elastic axis
x_β	nondimensional distance from the flap center of mass to the flap hinge
α	pitch rotation of the airfoil, measured about the elastic axis
α_f	α at the start of the freeplay region
β	angular rotation of flap about flap hinge
δ	length of the bilinear stiffness freeplay region
ζ_a	viscous damping ratio in pitch, $c_\alpha/2I_\alpha\omega_\alpha$
ζ_ξ	viscous damping ratio in plunge, $c_h/2m\omega_h$
μ	airfoil–air mass ratio, $m/\pi b^2$
ξ	nondimensional plunge displacement, h/b
τ	nondimensional time, tV/b
ω_ξ	uncoupled frequency ratio, ω_h/ω_α

and the response of the system is measured. Signal processing tools are used to obtain the frequency response function, which may be analyzed to find the natural frequencies, mode shapes and damping values for the aeroelastic system. These parameters can be used to predict the responses to various excitations and to improve the dynamic behavior of the system through design modification. Commonly used signal processing tools typically assume that the system is linear and the parameters time-invariant. The frequency response function obtained using these tools describes how the system responds to sinusoids at different frequencies, and is used to calculate modal damping values. The calculation of the frequency response function is based on the fact that a sinusoidal input to a linear system gives rise to a sinusoidal output at the same frequency as the input, although not necessarily at the same amplitude or in phase with it.

When these modal analysis techniques are applied to nonlinear dynamical systems, the results can be unexpected and accurate results for system frequency and damping values can be difficult to obtain. Nonlinearities in aeroelastic systems can arise from both structural and aerodynamic sources and may initiate aeroelastic instabilities well below the flutter speed predicted by linear theory. Typical nonlinear responses include limit cycle oscillations (LCOs) or, in some cases, chaotic response. One characteristic feature of nonlinear systems is that a single frequency excitation, such as a sinusoid, produces a multi-frequency response. In the case of a mechanical system, a sinusoidal input will generate a response (generally small) at multiples, or superharmonics, of the excitation frequency, even in systems that contain only slight nonlinearities. In the case of an aeroelastic system, it has been shown (Marsden and Price, 2001) that the introduction of a limited nonlinearity in one degree-of-freedom of a two degree-of-freedom aeroelastic system can cause distortion of the frequency response to a sine-sweep input. It has also been shown that this distortion can contribute to errors in the values of modal damping and frequency obtained using the frequency response function. These results provide the motivation for research towards a better understanding and predictive ability of the nonlinear content of aeroelastic response signals.

The spectrographic analysis technique is a signal-processing tool used in applications where the signal is not time-invariant, and where the frequency content as a function of time is important. Time–frequency spectrographic analysis is used in speech recognition and rotating machinery condition-monitoring applications (Cohen, 1989; Rohrbaugh, 1993). The technique has been used (Trickey et al., 2002) to study the frequency of LCOs as a function of airspeed. In the present study, the time-varying parameter is the frequency of the input force, allowing the input frequency/output frequency relationship over a range of frequencies to be studied using a single test at each airspeed.

2. Problem modelling

2.1. Aeroelastic system model

The structural contribution to the aeroelastic model consists of a two-dimensional typical section with three degrees-of-freedom as shown in Fig. 1. The airfoil is rigid and free to move in both the bending and pitch directions, while the flap is constrained to move only as required in order to apply the forcing input to the system. The airfoil structural flexibility is provided by torsional and translational springs in the pitch and plunge directions, respectively, while the flap has infinite stiffness and cannot respond to any internal or external forces. The aerodynamic model is linear using incompressible, inviscid and unsteady flow, and is limited to small amplitude oscillations about the equilibrium position.

A limited structural nonlinearity is introduced in the form of a bilinear torsional stiffness in the pitch direction. This type of nonlinearity is sometimes employed in aeroelastic analysis to represent a worn or loose control surface hinge. In this study, the particular case of a bilinear nonlinearity with zero central stiffness is investigated. This type of nonlinearity is often called freeplay or backlash, and the freeplay region may have preload ($m_0 \neq 0$) or no preload ($m_0 = 0$). The dimension of the freeplay region within the nonlinear torsional spring (δ) is chosen to be sufficiently large to allow the nonlinear presence to distort the system response, but not to overwhelm the "linear" shape of the resulting frequency response curve. The result is a system that is "globally" linear but contains an isolated nonlinearity that can appreciably affect the frequency response. The specific nonlinear restoring force used in this study, $M(\alpha(\tau))$ is shown in Fig. 2 and may be described by Eq. (1):

$$M(\alpha(\tau)) = \begin{cases} M_0 + \alpha(\tau) - \alpha_f & \text{for } \alpha \leqslant \dfrac{\sqrt{2}}{2}h - \left(1 + \dfrac{\sqrt{2}}{2}\right)\delta, \\ M_0 - r + \sqrt{r^2 - (\alpha(\tau) - h)^2} & \text{for } \dfrac{\sqrt{2}}{2}h - \left(1 + \dfrac{\sqrt{2}}{2}\right)\delta < \alpha(\tau) < -h, \\ M_0 & \text{for } -h \leqslant \alpha(\tau) \leqslant h \\ M_0 + r - \sqrt{r^2 - (\alpha(\tau) - h)^2} & \text{for } h < \alpha(\tau) < \left(1 + \dfrac{\sqrt{2}}{2}\right)\delta - \dfrac{\sqrt{2}}{2}h, \\ \alpha(\tau) - \alpha_f - \delta + M_0 & \text{for } \alpha(\tau) \geqslant \left(1 + \dfrac{\sqrt{2}}{2}\right)\delta - \dfrac{\sqrt{2}}{2}h. \end{cases} \tag{1}$$

Eq. (1) provides for highly localized continuous transitions between the linear portions of the restoring moment curve of Fig. 2. It has been shown (Marsden and Price, 2004) that this approximation provides a response signal with a frequency content similar to that of the discontinuous model.

The nondimensionalized equations of motion, obtained from Fung (1955) and modified to incorporate the nonlinear spring in the pitch degree-of-freedom are given in Eqs. (2) and (3):

$$\left(1 + \frac{1}{\mu}\right)\xi''(\tau) + \left(x_\alpha - \frac{a_h}{\mu}\right)\alpha''(\tau) + \left(\frac{m_\beta}{m}x_\beta - \frac{T_1}{\mu\pi}\right)\beta''(\tau) + \frac{1}{\mu}\alpha'(\tau) + 2\zeta_\xi\frac{\bar{\omega}_\xi}{U}\xi'(\tau) - \frac{T_4}{\mu\pi}\beta'(\tau) + \left(\frac{\bar{\omega}_\xi}{U}\right)^2\xi(\tau)$$
$$= -\frac{2}{\mu}\left\{C_1\phi(\tau) + \int_0^\tau \phi(\tau - \sigma)\lambda(\sigma)\,\mathrm{d}\sigma\right\}, \tag{2}$$

$$\left(\frac{x_\alpha}{r_\alpha^2} - \frac{a_h}{\mu r_\alpha^2}\right)\xi''(\tau) + \left(1 + \frac{1}{8\mu r_\alpha^2} + \frac{a_h^2}{\mu r_\alpha^2}\right)\alpha''(\tau) + \left(\frac{r_\alpha^2}{r_\beta^2} + \left[\frac{m_\beta}{m}\frac{x_\beta}{r_\alpha^2}(c_\beta - a_h)\right] - \frac{[T_7 + \{c_\beta - a_h\}T_1]}{\mu\pi r_\alpha^2}\right)\beta''(\tau)$$
$$+ \left(\frac{2\zeta_\alpha}{U} + \frac{(0.5 - a_h)}{\mu r_\alpha^2}\right)\alpha'(\tau) + \frac{1}{\mu\pi r_\alpha^2}(T_1 - T_8 - [c_\beta - a_h]T_4 + 0.5T_{11})\beta'(\tau)$$
$$+ \frac{(T_4 + T_{10})}{\mu\pi r_\alpha^2}\beta(\tau) + \frac{M(\alpha)}{U^2} = \frac{2}{\mu r_\alpha^2}(0.5 + a_h)\left[C_1\phi(\tau) + \int_0^\tau \phi(\tau - \sigma)\lambda(\sigma)\mathrm{d}\sigma\right]. \tag{3}$$

Eq. (2) is for the bending, or plunge degree-of-freedom and Eq. (3) is for the pitch direction. In both equations, ϕ represents Wagner's function and, when solving the equations numerically, is replaced with the approximation (Jones, 1940)

$$\phi(\tau) = 1 - 0.165\,\mathrm{e}^{-0.0455\tau} - 0.335\,\mathrm{e}^{-0.3\tau}.$$

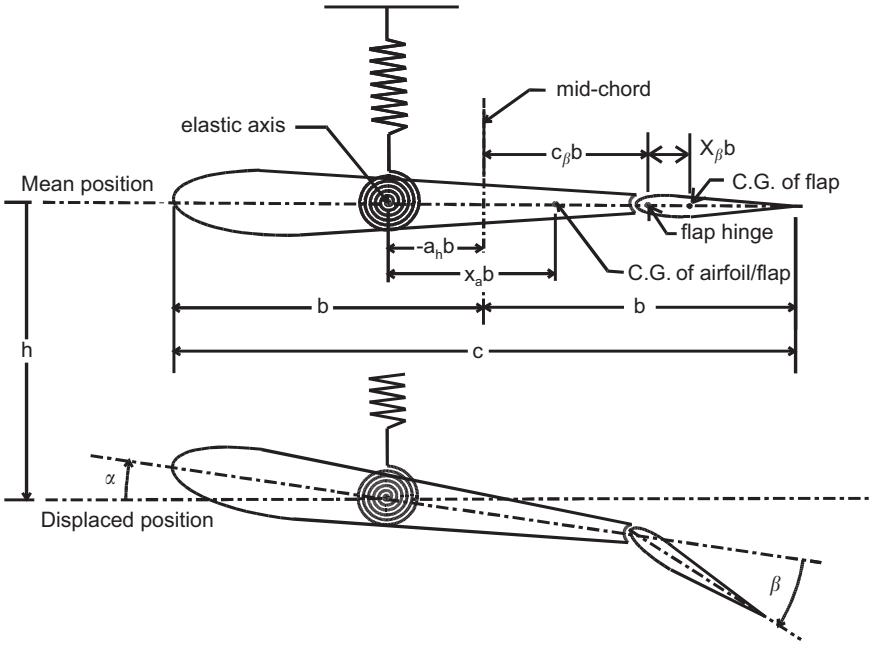

Fig. 1. Schematic of airfoil model.

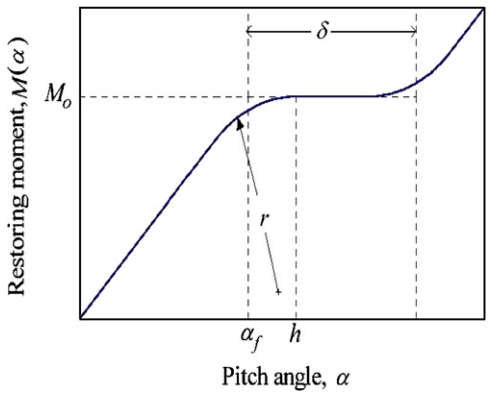

Fig. 2. Schematic of nonlinear restoring moment in pitch direction.

The equivalent linear system may also be described by Eqs. (2) and (3), except that the expression for the restoring force given in Eq. (1) is replaced by

$$M(\alpha(t)) = \alpha(t).$$

A sine-sweep excitation is applied to the system by constraining the flap motion to oscillate according to a specified schedule given by the following equation:

$$\beta(\tau) = \beta_0 \sin(\alpha\tau^2 + b\tau),$$

where the frequency of the input at any time τ is given by the expression

$$\omega(\tau) = 2a\tau + b. \tag{4}$$

The range of frequencies covered by the sine-sweep is chosen in order to include both the aeroelastic system natural frequencies.

The aeroelastic Eqs. (2) and (3) contain integral terms on the right-hand side, introduced by the unsteady aerodynamic theory, and may not be solved directly using standard numerical methods for ordinary differential

equations. In this study, the equations are reformulated as a set of eight ordinary differential equations (Alighanbari and Price, 1996). The resulting system of eight first-order differential equations is as given by

$$[A]\{X'\} + [B]\{X\} = \{F\}, \tag{5}$$

where

$$\{X\} = \{x_1, x_2, x_3, x_4, x_5, x_6, x_7, x_8\}^{\mathrm{T}},$$

$$\{F\} = \{0, 0, 0, 0, 0, 0, f_1(\tau), f_2(\tau)\}^{\mathrm{T}},$$

$$[A] = \begin{bmatrix} 1 & 0 & 0 & 0 & 0 & 0 & 0 & 0 \\ 0 & 1 & 0 & 0 & 0 & 0 & 0 & 0 \\ 0 & 0 & 1 & 0 & 0 & 0 & 0 & 0 \\ 0 & 0 & 0 & 1 & 0 & 0 & 0 & 0 \\ 0 & 0 & 0 & 0 & 1 & 0 & 0 & 0 \\ 0 & 0 & 0 & 0 & 0 & 1 & 0 & 0 \\ 0 & 0 & 0 & 0 & 0 & 0 & m_1 & m_2 \\ 0 & 0 & 0 & 0 & 0 & 0 & n_1 & n_2 \end{bmatrix}$$

and

$$[B] = \begin{bmatrix} 0 & 0 & -1 & 0 & 0 & 0 & 0 & 0 \\ 0 & 0 & 0 & -1 & 0 & 0 & 0 & 0 \\ 0 & 0 & 0 & 0 & -1 & 0 & 0 & 0 \\ 0 & 0 & 0 & 0 & 0 & -1 & 0 & 0 \\ 0 & 0 & 0 & 0 & 0 & 0 & -1 & 0 \\ 0 & 0 & 0 & 0 & 0 & 0 & 0 & -1 \\ m_{13} & m_{14} & m_{10} & m_{11} & m_7 & m_8 & m_4 & m_5 \\ m_{13} & n_{14} & n_{10} & n_{11} & n_7 & n_8 & n_4 & n_5 \end{bmatrix};$$

$f_1(\tau)$, $f_2(\tau)$, m_1 through m_{14}, and n_1 through n_{14}, are given in the Appendix A.

2.2. Simulation of airfoil response

Eq. (5) is solved to obtain time-histories of the airfoil motion in both the bending and pitch directions using a fourth-order Runge–Kutta numerical subroutine. The time step for the numerical integration was chosen to provide smooth derivatives up to the fourth order throughout the nonlinear region of the torsional spring. A more complete description of the methodology employed and results obtained is given in Marsden (2000).

3. Spectrographic analysis of the time-history response

The spectrographic analysis was performed on a sampling of the time-history records. A spectrograph was produced by separating the time-history data into equal-length overlapping segments and performing a Fast Fourier Transform (FFT) on each segment. The magnitude of the power spectra of the individual segments is then plotted as a function of time. For the results shown here, the time resolution interval between sample values within the data records was 0.5 nondimensional seconds (nds), with a record length of 1024 data points and an overlap of 512 data points. The choice of record length and time-resolution interval results in a Nyquist cut-off frequency of 2.0 rad/s. and a frequency resolution of 0.008 rad/nds. The spectrograph of the aeroelastic system response is a three-dimensional graphic, and may be presented in a number of ways. For the purpose of this study, it is the frequency content of the signal that is of primary interest, and the spectrographs are shown as contour plots looking down on the time/frequency plane. The time axis is labeled using the input frequency according to Eq. (4).

3.1. Linear and nonlinear frequency response

The frequency content of the linear and nonlinear responses can be compared by observing the spectrographs for the two output time-histories in the pitch degree-of-freedom. Figs. 3 and 4 compare the linear and nonlinear spectrographs, respectively, of the system response in pitch to a sine-sweep input at 93% of the linear flutter speed. The magnitude of the flap input, β_0, set to 2°, and the sweep rate is 0.000015 rad/nds, where nds stands for nondimensional second. The single, diagonal line of frequency response seen in Fig. 3 is typical of linear systems, with the output always at the same frequency as the input.

In contrast, the nonlinear frequency response shown in Fig. 4 is more complex. The diagonal line represents the linear portion of the nonlinear response where the output is at the same frequency as the input. This "linear" line divides the nonlinear frequency response into a superharmonic region in the upper left portion of the figure, and a subharmonic in the lower right-hand portion. The frequency response in Fig. 4 contains both sub- and superharmonic responses of two

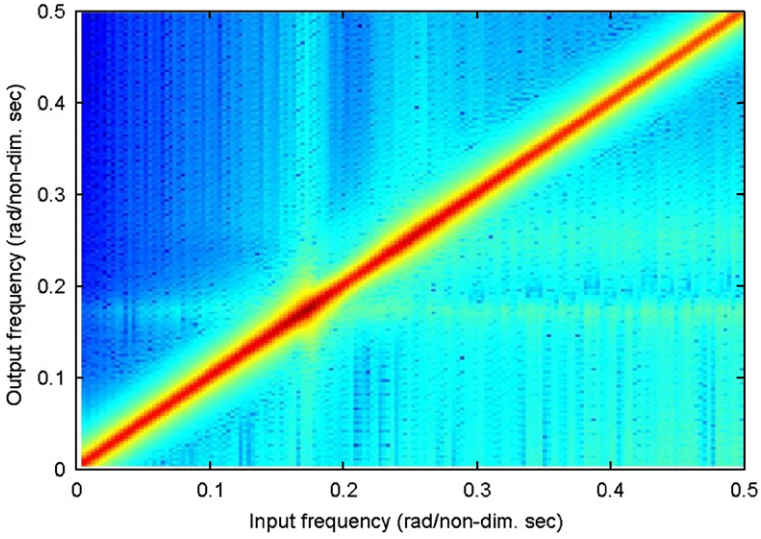

Fig. 3. Spectrograph of the linear system response to a sine-sweep input at 93% of the linear flutter speed.

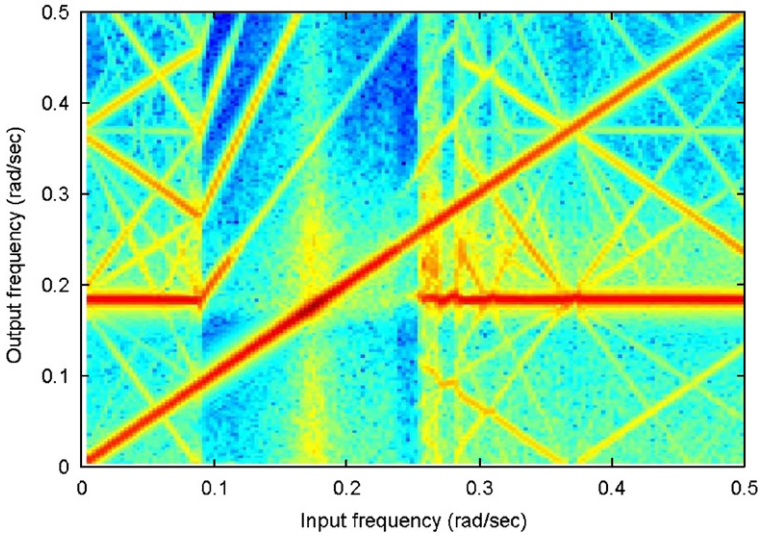

Fig. 4. Spectrograph of the nonlinear system response to a sine-sweep input at 93% of the linear flutter speed.

specific frequencies. The first is the input frequency and the second is a frequency that is independent of the input. The frequency response for the region between the input frequencies 0.90 and 0.25 rad/s is dominated by the input frequency and its integer-multiple superharmonics, while both above and below this range of input frequencies it is the second, constant frequency that dominates the output. In these two regions, the horizontal line of constant frequency response is superimposed on a relatively complex pattern of criss-crossing frequencies. This constant frequency, as will be discussed later, can be shown to be the LCO frequency for the aeroelastic response to a transient excitation.

Input/output frequency patterns similar to Fig. 4 can be obtained at almost all airspeeds above 50% of the linear flutter speed, but not for all values of input flap angle. For example, the spectrograph shown in Fig. 5 is similar to that of Fig. 4 and shows the frequency response pattern for the nonlinear system at 84% of the linear flutter speed, with β_0 equal to 1°. The pattern in Fig. 5 is even more complex than that of Fig. 4, with the frequency content of the response appearing as vertical bands of geometric patterns. Regardless of airspeed, all the frequency response patterns similar to those shown in Figs. 4 and 5 are a function of two frequencies: the input frequency and a single constant frequency represented by a horizontal band of frequency response. If the input frequency is designated as f_1, and the constant frequency as f_2, all the possible patterns shown in Figs. 4 and 5 may be represented by the following set of equations:

$$\pm if_1 \pm jf_2, \quad i = 0, 1, \ldots, C_1, \quad j = 0, 1, \ldots, C_2. \tag{6}$$

In Eq. (6), the values chosen for n and m will determine the range of frequencies covered by the pattern. Eq. (6) is plotted in Fig. 6 for $f_2 = 0.2$ rad/nds, $n = 3$ and $m = 5$. A comparison of Figs. 5 and 6 confirms that all the frequencies present in the response shown in Fig. 5 are also present in Fig. 6.

For almost all the input frequencies, the spectrograph of the aeroelastic system response to a sine-sweep input may be used to predict the response of the system to a single-frequency input. (In fact, at low values of input frequency this is not always true, and will be discussed later.) Fig. 7(a) and (b) show the power spectra of the system response to constant frequency inputs at 0.04 and 0.27 rad/nds, respectively, at 84% of the linear flutter speed. The frequencies in the response are the same as those appearing on the spectrograph of Fig. 5 at the corresponding input frequencies.

It is a useful result that the sine-sweep test as presented in this study may be used to efficiently predict the existence and frequency of LCOs, in the aeroelastic response of the system without any direct excitation apart from an initial displacement in one of its two degrees-of-freedom. It can be shown that the constant frequency band in the spectrograph, or f_2 in Eq. (6), is the LCO frequency for the aeroelastic system at that airspeed. Fig. 8(a) and (b) shows the time history and power spectrum, respectively, of the aeroelastic system response to an intial displacement in pitch at 84% of the linear flutter speed. The system responds with a LCO, at the frequency f_2 predicted by the sine-sweep test. It is of interest to note that this frequency is really a property of the aeroelastic system, and only a weak function of airspeed—a result that supports previous experimental work (Marsden and Price, 2005). The results also indicate that the frequency f_2 is essentially determined by the critical flutter speed of the equivalent linear system, with an additional dependence on airspeed. In the current study, the critical flutter frequency is approximately 0.18 rad/nds, and the LCO frequencies range from 0.18 rad/nds at 98% of the linear flutter speed to 0.27 rad/nds at 56% of the linear flutter speed.

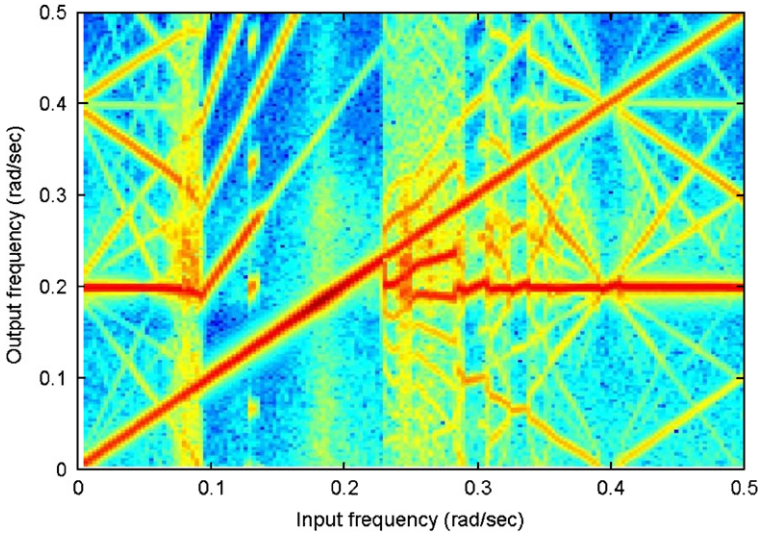

Fig. 5. Spectrograph of the nonlinear system response to a sine-sweep input at 84% of the linear flutter speed.

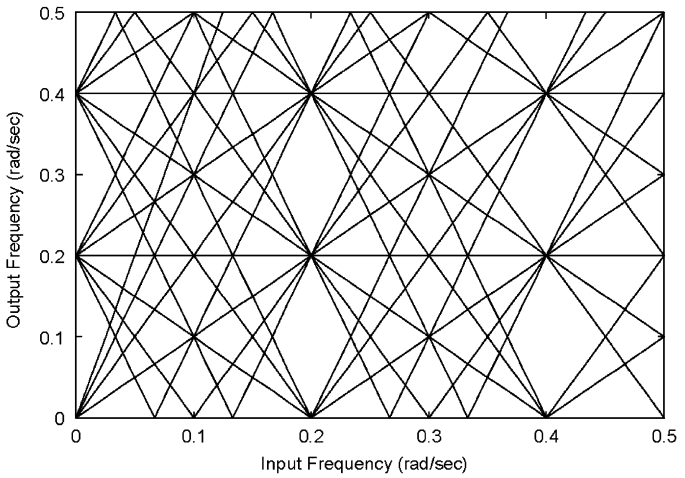

Fig. 6. Pattern of possible frequencies for the nonlinear system response to a sine-sweep input at 84% of the linear flutter speed calculated using Eq. (6) with $f_2 = 0.2$ rad/nds.

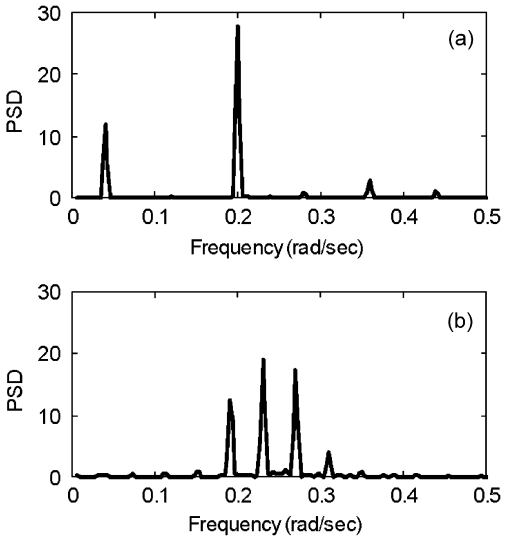

Fig. 7. Power spectra of the nonlinear system response to a constant frequency input at 84% of the linear flutter speed. (a) Input frequency 0.04 rad/nds and (b) 0.27 rad/nds.

3.2. Frequency response, LCO and amplitude of oscillation

One of the characteristics of nonlinear systems is that the frequency of the forced response, as well as the existence of LCOs in the free response, are functions of the amplitude of the response. The spectrographic analysis of the response to a sine-sweep input is an excellent tool for studying this phenomenon because as the input frequency sweeps across the range of natural frequencies of the system, the amplitude of the response varies considerably. It is clear that for very large amplitude responses, such as those in the resonant response near the first mode natural frequency (between 0.09 and 0.25 rad/nds in Fig. 5), the pattern of frequency response is different from the pattern in regions of lower amplitude response. In the regions of large amplitude response, the frequency content is limited to integer superharmonics of the forcing frequency, and in some cases to integer subharmonics with superharmonic + subharmonic content. For example (results not shown here), an input at frequency f_a will produce superharmonics at frequencies if_a, $i = 1, \ldots, n$, subharmonics at frequencies f_a/j, $j = 1, \ldots, m$, and combined harmonics at frequencies $if_a + f_a/j$, $i = 1, \ldots, n$, $j = 1, \ldots, m$. For the nonlinear system in this study, and the range of input frequencies shown in Figs. 4 and 5, n and m

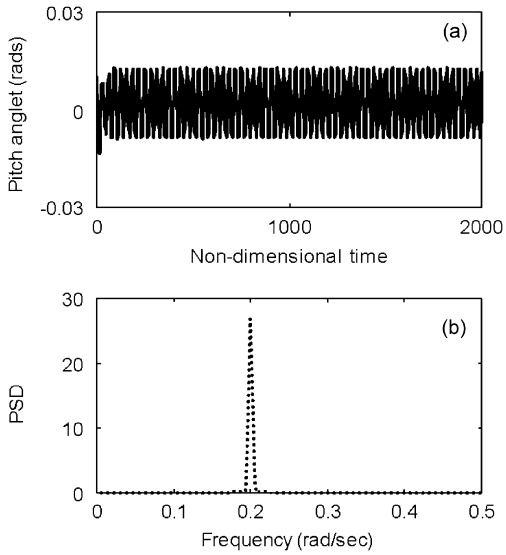

Fig. 8. Time history (a) and power spectrum (b) of the nonlinear system free response in the pitch degree-of-freedom to an initial displacement in pitch at 84% of the linear flutter speed.

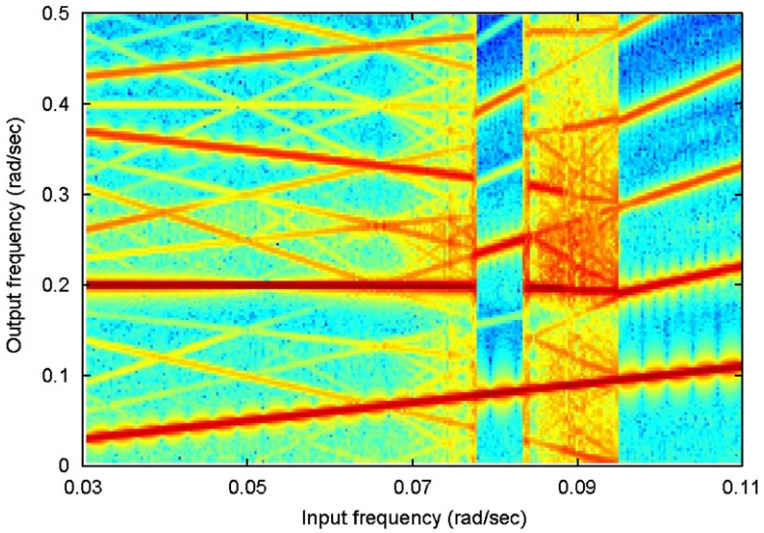

Fig. 9. Spectrograph of the nonlinear system response to a sine-sweep input at 84% of the linear flutter speed. Sweep rate 0.00000015 rad/nds, sweep begins at 0.03 rad/nds.

are limited to 3. Although the number of super- and subharmonic frequencies present in this type of response may or may not be a function of amplitude, this is not obviously the case, and the question requires more study.

The spectrographic analysis of the sine-sweep raises questions concerning the amplitude dependence of the frequency response of the nonlinear aeroelastic system. A comparison of the spectrograph of the frequency response with the amplitude of the time-history response (not shown) reveals a range of amplitudes for which the frequency responses are quite different. The frequency response at two different input frequencies may produce the same amplitude of response, but not with the same frequency content. In addition, two sine-sweeps with the same magnitude of forcing function but different sweep rates, or starting at different frequencies can produce different output frequencies. This is particularly true at low values of frequency below the first mode natural frequency. As an example, Figs. 9 and 10 both show the frequency response to a sine-sweep input at 0.00000015 rad/nds, at 84% of the linear flutter speed. The response in

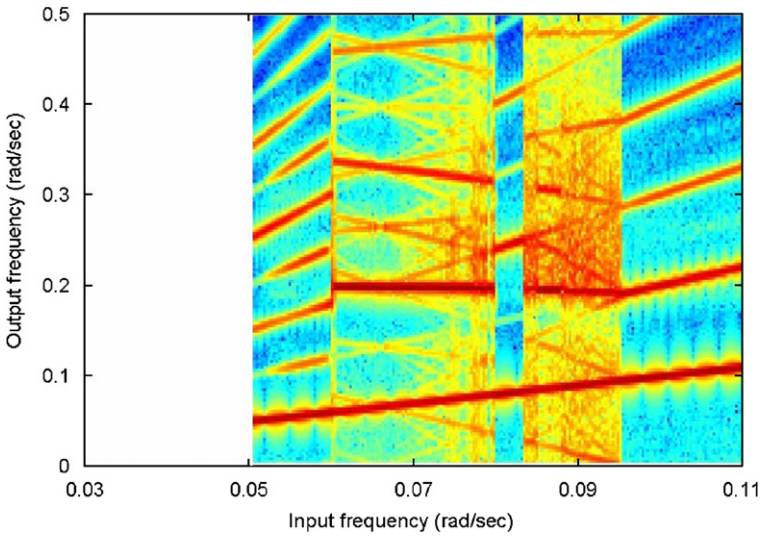

Fig. 10. Spectrograph of the nonlinear system response to a sine-sweep input at 84% of the linear flutter speed. Sweep rate 0.00000015 rad/nds, sweep begins at 0.05 rad/nds.

Fig. 9 is to a sine-sweep starting at 0.03 rad/nds, while the response in Fig. 10 is to a sine-sweep starting at 0.05 rad/nds. The vertical band of integer frequency responses between 0.07 and 0.09 rad/nds input frequencies is wider in Fig. 9 than in Fig. 10, and the frequency content at the beginning of the sine sweep seen in Fig. 10 is absent from Fig. 9. These preliminary results imply that the frequency response is more likely to be a function of phase angle than amplitude. It seems possible that the amplitude of the response is a factor affecting the phase angle within the freeplay region, but that it is the phase angle that ultimately determines the frequency response in the case of the forced response, or the existence of LCO for the free response.

4. Conclusion

The results presented suggest the following conclusions regarding the use of the spectrographic analysis method for the study of the structurally nonlinear aeroelastic system.

(i) Spectrographic analysis, when combined with a sine-sweep excitation, is an efficient and productive tool for investigating the response of the nonlinear aeroelastic system.
(ii) This type of analysis yields information about the forced response and the response without direct excitation of the nonlinear system within the context of a relatively simple test.
(iii) All the frequencies that may be present in the frequency response of the structurally nonlinear system with freeplay to a forced excitation may be generated as a simple function of two fundamental frequencies.
(iv) The frequency and existence of an LCO in the aeroelastic response of the system without direct excitation at any particular airspeed may be determined from the spectrograph of the sine-sweep response.
(v) Results suggest that the frequency response and existence of LCO for this type of nonlinear aeroelastic system may be a function of phase angle in the freeplay region.

The usefulness of this technique for nonlinear aeroelastic system analysis will require further study, in particular oriented toward a better understanding of the relationship between the input frequency and the different patterns of output frequencies. At slow sweep-rates and low values of input frequency, the frequency response pattern is dependent on the sweep-rate and the starting frequency. At faster sweep-rates and higher input frequency, although the pattern appears to be amplitude-dependent, it can be shown that this is not always the case. Additional investigation may reveal which specific parameters contribute to the changing patterns of output frequency. In addition, it would be of interest to compare the content and pattern of the frequency responses seen in this study with those obtained for other types of nonlinearities, such as cubic stiffness or damping.

Acknowledgment

The authors acknowledge the support by the Natural Sciences and Engineering Research Council (NSERC) of Canada.

Appendix A

Expressions from Eq. (5) are:

$$f_1(\tau) = -m_3\beta''''(\tau) - m_6\beta'''(\tau) - m_9\beta''(\tau) - m_{12}\beta'(\tau) - m_{15}\beta(\tau),$$

$$f_2(\tau) = -\frac{bd}{U^2}M(\alpha(\tau)) - \frac{b+d}{U^2}M'(\alpha(\tau)) - \frac{M''(\alpha(\tau))}{U^2} - n_3\beta''''(\tau) - n_6\beta'''(\tau) - n_9\beta''(\tau) - n_{12}\beta'(\tau) - n_{15}\beta(\tau);$$

$$m_1 = 1 + \frac{1}{\mu}, \quad m_2 = x_\alpha - \frac{a_h}{\mu}, \quad m_4 = 2\zeta_\xi\frac{\bar{\omega}_\xi}{U} + (b+d)\left(1+\frac{1}{\mu}\right) + \frac{2}{\mu}(1-a-c),$$

$$m_5 = \frac{1}{\mu} + (b+d)\left(x_\alpha - \frac{a_h}{\mu}\right) + \frac{2}{\mu}(0.5-a_h)(1-a-c), \quad m_7 = \left(\frac{\bar{\omega}_\xi}{U}\right)^2 + bd\left(1+\frac{1}{\mu}\right) + 2(b+d)\zeta_\xi\frac{\bar{\omega}_\xi}{U} - \frac{2}{\mu}(ad+cb-b-d),$$

$$m_8 = bd\left(x_\alpha - \frac{a_h}{\mu}\right) + \frac{b+d}{\mu} + \frac{2}{\mu}(1-a-c) - \frac{2}{\mu}(0.5-a_h)(ad+bc-b-d),$$

$$m_{10} = 2bd\zeta_\xi\frac{\bar{\omega}_\xi}{U} + (b+d)\left(\frac{\bar{\omega}_\xi}{U}\right)^2 + \frac{2}{\mu}bd,$$

$$m_{11} = \frac{bd}{\mu} - \frac{2}{\mu}(ad+cb-b-d) + \frac{2}{\mu}bd(0.5-a_h), \quad m_{13} = bd\left(\frac{\bar{\omega}_\xi}{U}\right)^2, \quad m_{14} = \frac{2bd}{\mu};$$

$$n_1 = \frac{1}{r_\alpha^2}\left(x_\alpha - \frac{a_h}{\mu}\right), \quad n_2 = \frac{1}{\mu r_\alpha^2}\left(\mu r_\alpha^2 + \frac{1}{8} + a_h^2\right),$$

$$n_4 = \frac{x_\alpha}{r_\alpha^2}(b+d) - \frac{a_h}{\mu r_\alpha^2}(b+d) - \frac{2}{\mu r_\alpha^2}(0.5+a_h)(1-a-c),$$

$$n_5 = \frac{2\zeta_\alpha}{U} + \frac{(0.5-a_h)}{\mu r_\alpha^2} + \frac{(b+d)}{\mu r_\alpha^2}\left(\mu r_\alpha^2 + \frac{1}{8} + a_h^2\right) - \frac{2}{\mu r_\alpha^2}(0.5+a_h)(1-a-c)(0.5-a_h),$$

$$n_7 = \frac{bdx_\alpha}{r_\alpha^2} - \frac{bda_h}{\mu r_\alpha^2} - \frac{2}{\mu r_\alpha^2}(0.5+a_h)(b+d-ad-bc),$$

$$n_8 = \frac{bd}{\mu r_\alpha^2}\left(\mu r_\alpha^2 + \frac{1}{8} + a_h^2\right) + \frac{2}{\mu}(b+d)\zeta_\alpha + \frac{b+d}{\mu r_\alpha^2}(0.5-a_h) - \frac{2}{\mu r_\alpha^2}(0.5+a_h)(0.5-a_h)(b+d-ad-bc) - \frac{2}{\mu r_\alpha^2}(0.5+a_h)(1-a-c),$$

$$n_{10} = -\frac{2bd}{\mu r_\alpha^2}(0.5+a_h),$$

$$n_{11} = \frac{2bd}{U}\zeta_\alpha + \frac{bd}{\mu r_\alpha^2}(0.5 - a_h) - \frac{2bd}{\mu r_\alpha^2}(0.5 + a_h)(0.5 - a_h) - \frac{2}{\mu r_\alpha^2}(0.5 + a_h)(b + d - ad - bc),$$

$$n_{13} = 0, \quad n_{14} = -\frac{2bd}{\mu r_\alpha^2}(0.5 + a_h).$$

References

Alighanbari, H., Price, S.J., 1996. The post-Hopf-bifurcation response of an airfoil in incompressible two-dimensional flow. Nonlinear Dynamics 10, 381–400.

Cohen, L., 1989. Time–frequency distributions—a review. Proceedings of the IEEE 77, 941–981.

Fung, Y.C., 1955. An Introduction to the Theory of Aeroelasticity. Wiley, New York.

Jones, R.T., 1940. The unsteady lift of a wing of finite aspect ratio. NACA Report 681.

Marsden, C.C., 2000. Identification of aeroelastic parameters using sweep excitation. M. Eng. Thesis. McGill University, Montréal, Que., Canada.

Marsden, C.C., Price, S.J., 2001. Modal damping identification for a structurally nonlinear airfoil using sweep excitation. In: Proceedings of the 42nd AIAA/ASME/ASCE/AHS/ASC Structures, Structural Dynamics, and Materials Conference and Exhibit, pp. 3008–3018.

Marsden, C.C., Price, S.J., 2004. Equivalent linear modal parameter estimation for a nonlinear aeroelastic system. Journal of Fluids and Structures 19, 607–619.

Marsden, C.C., Price, S.J., 2005. The aeroelastic response of a wing section with a structural freeplay nonlinearity: an experimental investigation. Journal of Fluids and Structures 21, 257–276.

Rohrbaugh, R.A., 1993. Application of time–frequency analysis to machinery condition assessment. Conference Record of the Asilomar Conference on Signals, Systems & Computers 7, pp. 1455–1458.

Trickey, S.T., Virgin, L.N., Dowell, E.H., 2002. The stability of limit-cycle oscillations in a nonlinear aeroelastic system. Proceedings of the Royal Society London 458, 2203–2226.